



# Identification and investigation of martian dust source regions from orbital observation



Laura Kulowski<sup>1</sup> & Huiqun Wang<sup>2</sup>

<sup>1</sup>Brown University, Providence, RI, USA

<sup>2</sup>Harvard-Smithsonian Center for Astrophysics, Cambridge, MA, USA

## Introduction

We have constructed a database of locations of active dust lifting from existing Mars Daily Global Maps (MDGMs) generated by Mars Global Surveyor's Mars Orbiter Camera. This database includes information on lifting that occurs between 60°N and 60°S and between Mars Years 24 and 27 (July 1999 - January 2005). In order to get the statistics for "normal" Martian conditions, we have concentrated on the periods without global dust storms. In this poster, we outline our visual method for identifying active dust lifting, which is based on an analysis of albedo changes, color, and morphology. Using this database, we assess the spatial, temporal, and size distribution of lifting areas with attention to lifting structures. We also compare our results with the surface wind stress and dust deposition patterns predicted by various Mars General Circulation Models.

## Identification of Active Dust Lifting

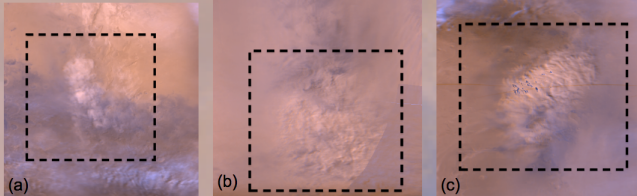


Figure 1. Three examples of active dust lifting are enclosed in the dashed boxes. Lifting in panel (a) has a puffy structure, panel (b) has a pebbled structure, and panel (c) has a plume structure.

Our method to identify areas of active dust lifting comprises four steps:

- (1) Consecutive MDGMs are examined for **albedo variations**.
- (2) Maps that show albedo variations are examined for **orange or red** dust storms.
- (3) Maps that fit the albedo variations and color constraints are analyzed for **structures** associated with dust lifting (convective lobes, mottled appearance).
- (4) Areas of dust lifting are manually **marked** in the MDGM and **stored** in an object containing information about the size, location, time, and structure of the event.

We have defined three morphological classifications, puffy, pebbled, and plume, to describe the different morphologies observed in MDGMs (Figure 1).

## Size Distribution

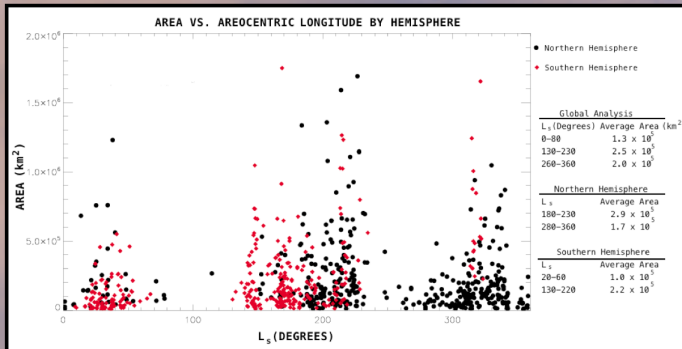


Figure 2. Lifting tends to occur in three seasonal windows:  $L_s = 0^\circ\text{-}80^\circ$ ,  $L_s = 130^\circ\text{-}230^\circ$ , and  $L_s = 260^\circ\text{-}360^\circ$ . These last two time periods are included in the traditional dust lifting season. Northern and southern events each have their own preferred seasonal windows of occurrence. Northern ones are concentrated during  $L_s=180^\circ\text{-}230^\circ$  and  $L_s=280^\circ\text{-}360^\circ$  and southern ones concentrated during  $L_s=20^\circ\text{-}60^\circ$  and  $L_s=130^\circ\text{-}220^\circ$ .

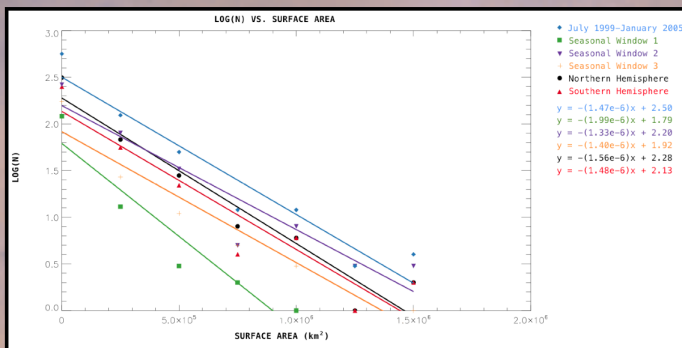


Figure 3. Small lifting events are much more common than large lifting events. The rapid decay of the number of events with increasing area is observed for all seasonal windows ( $L_s=0^\circ\text{-}80^\circ$ ,  $L_s=130^\circ\text{-}230^\circ$ , and  $L_s=260^\circ\text{-}360^\circ$ ) and in each hemisphere. Note that the first seasonal window, which occurs outside the dusty season, has the most severe decay rate.

## Acknowledgements

L. Kulowski is supported by the National Science Foundation Research Experiences for Undergraduates (REU) and Department of Defense ASSURE programs under NSF Grant no. 1262851 and by the Smithsonian Institution. H. Wang is supported by NASA's Mars Data Analysis Program. Thanks to J. McDowell, M. Machacek, and Z. Slepian for their helpful discussions.

## Frequency Distribution

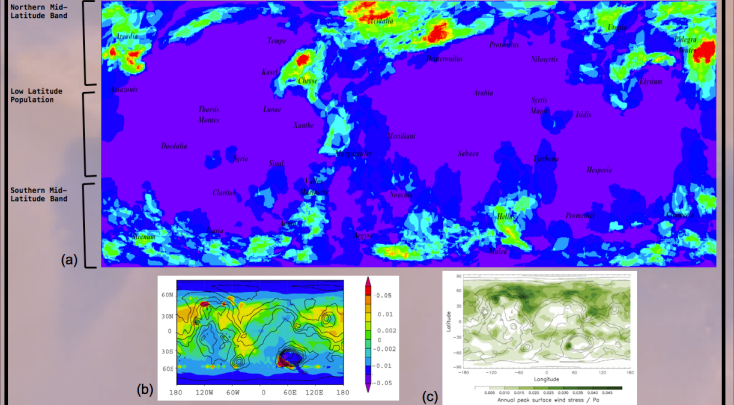


Figure 4. (a) The highest frequency lifting occurs in the northern mid-latitude band. The low latitude population has a highly asymmetric frequency distribution, with lifting concentrated in topographic lows. The most symmetric distribution of lifting occurs in the southern mid-latitude band. Annual maximum surface wind stress provided by (b) Basu et al. and (c) Mulholland et al. predict high wind stress in Arcadia, Acidalia, Cebrenia, and Hellas. These locations correspond well with our high frequency lifting areas. Tharsis, Arabia, and Elysium are net dust deposition areas, which is also in agreement.

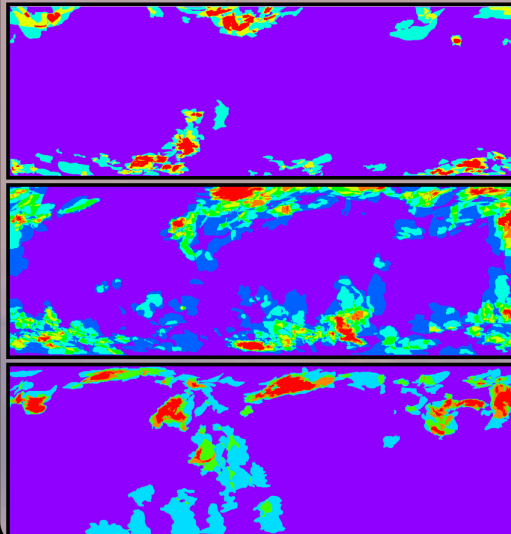


Figure 5. Frequency distribution for  $L_s=0^\circ\text{-}80^\circ$ . Note that the northern and southern mid-latitude bands are the most active. The low latitude population is relatively inactive.

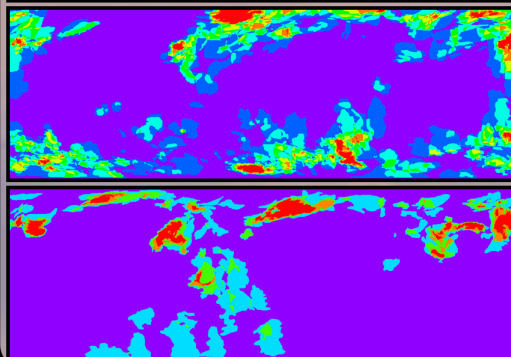


Figure 6. Frequency distribution for  $L_s=130^\circ\text{-}230^\circ$ . This is the most active seasonal window. Note that Hellas basin becomes active and southern activity has the greatest zonal symmetry.

## Morphological Properties

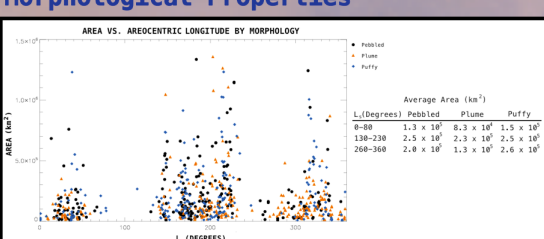


Figure 7. Frequency distribution for  $L_s=260^\circ\text{-}360^\circ$ . The northern mid-latitude band has similar behavior to that during  $L_s=130^\circ\text{-}230^\circ$ . Note that Hellas is no longer active and southern activity is much less active.

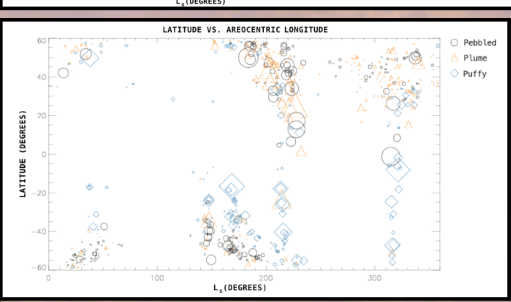


Figure 8. Area of each lifting event as a function of areocentric longitude. Puffy, pebbled, and plume structures show no seasonal preference and are apparent in all seasonal windows. Puffy and pebbled morphologies tend to be larger than plume morphologies.

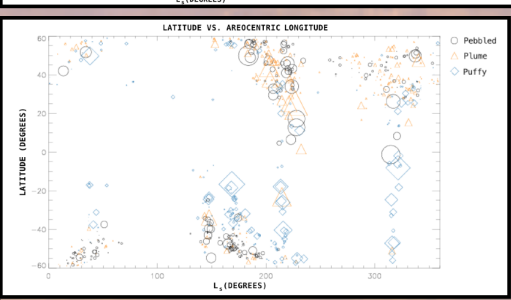


Figure 9. Latitudinal distribution of puffy, pebbled, and plume morphologies as a function of areocentric longitude. The size of each symbol is proportional to the area of the lifting event. This plot indicates that dust lifting is more common at higher latitudes, reinforcing our frequency distribution observations. Pebbled and plume structures tend to occur at higher latitudes while puffy structures occur at both high and low latitudes.